Corrugated Cardboard Core Sandwich Beams with Bio-Based Flax Fiber Composite Skins

Aidan McCracken and Pedram Sadeghian[1]

Department of Civil and Resource Engineering, Dalhousie University, Halifax, NS, B3H 4R2, Canada.

ABSTRACT

This paper presents an experimental study on the behavior of sandwich beams made of green materials for both core and skin components. A unidirectional flax fabric and a partial bio-based epoxy were used to make fiber-reinforced polymer (FRP) skins and three flute varieties of corrugated cardboards (known as B, C, and BC flutes) with the bulk densities of 170, 127, and 138 kg/m^3 were used for the core, respectively. A total of 30 small-scale sandwich beam specimens were manufactured across six unique beam varieties with dimensions of 50 mm in width, 25 mm in depth, and 200 and 350 mm in length (150 mm and 300 mm spans) and tested under four-point bending up to failure. Two failure modes of transverse indentation for the short specimens and longitudinal crushing of the core and skin for the long specimens were observed. The load-deflection, load-strain, and moment-curvature behaviors were analyzed to evaluate the strength and stiffness of the sandwich beam specimens. C flute with the lowest bulk density and the highest availability in the market amongst all the three flutes exhibited the highest strength and stiffness for sandwich applications. Overall, the corrugated cardboard cores combining with the flax FRP skins may be considered as a viable, green option for the fabrication of large-scale structural sandwich panels for building applications.

---

[1] Corresponding Author: Pedram.Sadeghian@dal.ca

KEYWORDS: Corrugated Cardboard, Flax FRP, Bio-Based Polymer, Green, Sandwich.

1. INTRODUCTION

Composite sandwich structures made of fiber-reinforced polymer (FRP) skins and lightweight, low-density core materials have been shown to be very effective in reducing weight and increasing strength and stiffness in a variety of construction and building applications. The FRP skins resist the tensile and compressive stresses under flexure, like the action of the flanges on an I-shaped beam, while the core resists shear stresses, increases the distance between skins resulting in a higher moment of inertia, and provides insulation for the system. The popularity of sandwich structures in the form of wall, cladding, roof, and floor panels is growing as engineers look to improve the structural efficiency and insulation properties of buildings. To be more environmentally-conscious, conventional materials and structures need be re-evaluated to determine how they can become more sustainable and have a smaller environmental impact during manufacturing, installation, and service.

Although FRP composites made of synthetic fibers, such as glass or carbon fibers, are often used for the skins of sandwich panels [1][2][3], the concept of using plant-based natural fibers, such as flax and hemp fibers, has also been explored [4][5][6]. Although the natural fibers have a lower strength than their synthetic counterparts, it has been showed that this may be acceptable since the core failure is one of common failure modes in sandwich structures with strong skins [7][8]. However, sandwich structure may experience different failure modes (core shear, indentation, skin crushing/rupture, and skin wrinkling) dependent on the ratio of skin thickness to span length and relative core density [9][10]. Additionally, natural fibers have many economic and environmental advantages compared to synthetic fibers [11][12][13]. Thus, FRP skins made of

natural fibers represent a viable structural option for sandwich structures and are a more environmentally-friendly choice than synthetically produced fibers. In FRPs, the role of polymer resins to impregnate and bond the fibers is critical. Synthetic polymers, such as epoxy and vinyl ester, have been used with natural fibers [14][15][16]. However, numerous studies have been conducted on the use of fully or partially bio-based resins with natural fibers [17][18]**Error! Reference source not found.**.

Beside of skin materials, the core materials of sandwich structures play a major role in the structural (i.e. shear, composite action, and out-of-plane properties) and insulation properties. Many different core materials have been explored for use in sandwich structures. Core materials that are commonly studied include low-density foam and plastic or metal honeycombs [20][21][22]. To present a more sustainable option, this study considers corrugated cardboard as the core material. According to the Paper and Paperboard Packaging Environmental Council (PPEC), approximately 85% of corrugated cardboard in Canada is recycled and new cardboard is produced with nearly 100% recycled materials [25][22]. Along with being 100% biodegradable, corrugated cardboard is a very sustainable as it can be repurposed and produces very little waste. Corrugated cardboard is an orthotropic sandwich with two paper based facings separated by a lightweight corrugated core known as fluting [23]. The system has good thermal insulation properties and high load-carrying capacity by being low-costs and lightweight [24]. Although studies have been conducted on balsa wood and cork cores for sandwich composites [4][5][26][27], corrugated cardboard has not been explicitly studied in the context of a sandwich composites with natural fibers and bio-based resins.

In this study, flax FRP skins were combined with corrugated cardboard cores to manufacture sandwich beam specimens. Unidirectional flax fabrics were impregnated using a resin

with almost 30% bio content. As a result, the sandwich beams produced were constructed using almost entirely green materials. The aim of the study is to analyze and evaluate the structural performance of corrugated cardboard and flax FRP sandwich beams as an alternative to conventional construction and building materials. Although flax has previously studied for use in sandwich beams, the combination of flax FRP with cardboard has yet to be analyzed. This combination of materials represents a structural system that has a minimal impact on the environment as corrugated cardboard is readily available and composed almost entirely of recycled and green material.

2. EXPERIMENTAL PROGRAM

This section presents the details of test matrix, material properties, specimen preparation, test setup, and instrumentation of the test specimens. The experimental program using two loading arrangements was specifically designed to investigate the properties of three corrugated cardboard cores.

2.1. Test Matrix

A total of 30 flax FRP and corrugated cardboard sandwich beams were fabricated to be tested in four-point bending. All specimens were constructed using one layer of flax FRP skin on either side and a corrugated cardboard core with a thickness of approximately 25 mm. The variables being tested were span length as well as the flute sizes of the corrugated cardboard. Two span lengths of 150 mm and 300 mm as well as three flute sizes of B, C, and BC were tested. More information concerning the flute sizes can be found in the next section. A complete summary of this study's test matrix is shown in Table 1. Note that three identical specimens were manufactured and tested per case. All specimens are identified with a specimen identification (ID) which follows the format X-SY where X identifies the flute size, S stands for span and Y identifies the specimens test span

in mm. For example, the specimen B-S150 designates a flax FRP and cardboard sandwich beam constructed using B flute cardboard with a test span length of 150 mm.

2.2. Material Properties

Three unique carboard flutes were used in the fabrication of the sandwich beams: B, C and BC flutes. Cardboard flutes are standard in international packing and are identified with a single capital letter. Each flute has a different nominal thickness and density. Table 2 compares the approximate measured dimensions of each flute in this study. The density measurements were taken after the flute layers had been combined into a core for the specimens. Thus, this density reflects the actual density of the core, including the small amount of starch-based adhesive used to combine the layers of cardboard.

Figure 1 shows a visual comparison between the flutes with both a photo of the flutes as a part of a core as well as a 2D side-view schematic. For the flax FRP skins, a unidirectional flax fabric with a reported aerial weight of 275 g/m^2 (gsm) was used. In terms of epoxy, Super Sap ONE was used, which is a bio-based epoxy (30% bio content) with a reported tensile strength, modulus and elongation of approximately 53.23 MPa, 2.65 GPa and 6 %, respectively. Betts et al. [26] conducted a study on the tensile properties of flax FRP composites manufactured using the same unidirectional flax fabric and three different epoxies. For the flax FRP samples made of the bio-based epoxy used in this study, the average tensile strength and initial modulus were reported to be 198.0 ± 9.3 MPa and 17.09 ± 0.63 GPa, respectively (two-layer thickness = 1.97 ± 0.09 mm). A secondary modulus was reported as 11.93 ± 0.39 GPa as it was found flax FRPs display an approximately bi-linear mechanical behavior. The rupture strain of flax FRP was reported to be 0.0153 ± 0.0006 mm/mm.

2.3. Specimen Preparation

The first step in the fabrication of the sandwich beams was to construct the cardboard cores. To do this, strips of cardboard (manufacturer: Maritime Paper, Dartmouth, NS, Canada) approximately 25 mm in width were cut from larger sheets using a straight edge and a sharp blade. The two span lengths being tested were 150 and 300 mm, thus strips were cut to lengths of 200 and 350 mm to provide an overhang of approximately 25 mm on each end of the specimen. To bond the strips together, a small amount of a vegetable starch-based adhesive known as Tri-Tex Tribond P-1031 adhesive was used. This adhesive was provided by the cardboard manufacturer and is the same used in the manufacturing of corrugated cardboards. The number of strips in the core varied per flute as all cores were manufactured to have an approximate width of 50 mm. Figure 2 shows the fabrication process of the cardboard cores.

Once the cardboard cores were completed, the flax FRP skins were applied using the standard wet lay-up method. Sheets of flax fabrics approximately 300 mm in width and either 200 or 350 mm in length were pre-cut before the mixing of the epoxy. A sheet of parchment paper was put on the bottom surface and a layer of epoxy was applied. Next, a sheet of flax fabric was applied to the epoxy, then the top side of the fabric was saturated with another layer of epoxy. Each of the five cores per case was placed on the saturated sheet of flax. A piece of particle board was placed on top of the cores while the bottom layer of flax FRP cured. Once the first side of had cured, this process was repeated for applying the flax FRP skin to the other side of the cores. This method allowed for the curing FRP to always be below the cardboard core to help ensure that unwanted resin did not seep down into the cardboard. Figure 3 shows the application process of the second side of flax FRP. Applying larger sheets of flax fabric allowed for a quicker fabrication process. Once both sides fully cured, a bandsaw was used to cut the beams to their approximate width of

50 mm and a rotary sander was used to smooth the edges of the flax composite and ensure it was in line with the sides of the core. A completed sandwich beam is shown in Figure 4.

2.4. Test Setup and Instrumentation

The test setup was designed based on ASTM D7250 [29] to test each type of sandwich beams with two different loading arrangements towards obtaining the flexural stiffness and shear stiffness. All specimens were tested under four-point bending per with a loading span proportional to the supporting spans of 150 and 300 mm. The loading span (L) was selected to be equal to (2/11) of the supporting span (S). A schematic of the four-point bending setup is shown in Figure 5, where P is the total applied load. In terms of instrumentation, a strain gauge was applied on either side of the sandwich beam, centered in the longitudinal direction to measure the tensile and compressive strains. Additionally, two linear potentiometers (LPs) were setup in the middle of the beam's span to measure an average mid-span deflection. These values, along with the applied load, measured every 0.1 seconds, were collected for data processing. All tests were completed using a 100 kN universal testing machine and were displacement controlled using a fixed rate of 2 mm/min.

3. TEST RESULTS AND DISCUSSION

This section presents the derails of failure mode, load-strain, moment-curvature, load-deflection, and flexural and shear stiffness of the test specimens. A summary of the test results as well as the modes of failure of the specimens is shown in Table 3.

3.1. Failure Modes

As expected, the failure of the core was the initial source of failure in both the 150 and 300 mm span sandwich beams. Due to their higher stiffness, the 150 mm span specimens did not flex very much, only deflecting and average of 3.37 mm at peak load. All three tested 150 mm specimens

failed by indentation crushing of the core due to the transverse loads. This was followed by indentation of the top skin. However, the 300 mm span specimens reached a significantly lower peak load and failed by longitudinal crushing of the core due to compressive bending stresses. Once the corrugated cardboard begun crushing longitudinally, this created a noticeable increase in compressive strain on the top of the beam, which caused the top skin to be crushed after the peak load. Images of these two failure modes can be seen in Figure 6.

3.2. Load-Strain Behavior

The longitudinal strains of top and bottom skins at mid-span of each specimen were recorded. Curves comparing the load-strain behavior of the specimens are shown in Figure 7. Each curve is the average of three identical specimens of each group of specimens. The 300 mm span specimens experienced much larger compressive strain compared to tensile strain. This was caused by the longitudinal crushing of the cardboard near the top skin of the sandwich. The 150 mm span samples experienced comparable tensile and compressive strains until the indentation crushing of the cardboard core. Overall, the specimens with B and C flutes showed better performance than the specimens with BC flute. The load-strain behavior of the 150 mm span specimens with B and C flutes were very close at the tension side until around the peak load. However, at the compression side, the strain of specimens with B flute went more non-linear. As the tensile rupture strain of flax FRP was about 0.015 mm/mm based on tensile coupon tests, it can be seen that only the 150 mm span specimens with B and C flutes reached to that level of strain, however the specimens failed by indentation of compression side under the load. In the 300 mm span specimens, the strain of tensile skins of B and C flutes reached to 0.013 and 0.009 mm/mm, which are slightly less than the tensile rupture strain of 0.0153 mm/mm. This shows that the two cardboards core were strong and stiff enough to develop that level of tensile strains. At the compression side, the flax FRP skins

of both B and C flutes experienced a maximum compressive strain of almost 0.014 mm/mm before the load dropped. Overall, B and C flutes showed compatible strength and stiffness to the flax FRP skins.

3.3. Moment-Curvature Behavior

The moment in the central loading span of each specimen was calculated at any load level. The curvature of each specimen was also calculated based on the slope of strain profile at mid-span. The strain profile was assumed linear and obtained using the tensile and compressive strains of skins discussed earlier. As expected, the moment-curvature behavior was similar between the two spans that were compared. Graphs comparing the moment-curvature behavior of the specimens are shown in Figure 8. The specimens with 150 mm span and B and C flutes exhibited very close moment-curvature behavior with almost the same ultimate curvature. Both the specimen groups, showed significantly better performance than the specimens with BC flute. As the specimens with 300 mm span failed due to flexure, moment-curvature curves are more applicable explaining the behavior of these specimens. As shown in Figure 8, the specimens with C flute exhibited a higher flexural stiffness and strength than those with B and BC flutes. Flexural stiffness of the specimens was calculated based on the slope of the linear region of each curve and presented in Table 3. The results will be discussed further in Section 3.5.

3.4. Load-Deflection Behavior

The mid-span deflection of each specimen was obtained by averaging the displacement data from the two LPs installed on the bottom skin. Each load-deflection curve in Figure 9 represents the average load-deflection curves of three identical specimens of each group. The figure indicates that both 150 and 300 mm span specimens experienced a short linear behavior followed with a long non-linear region up to the peak load. The initial stiffness K of each specimen was calculated

base don the slop of the linear region. As shown in Table 3, the initial stiffness of the specimens with different flutes are close to each other, however the specimens with BC flute failed at much lower load than those with B and C flutes. The conventional deflection limit of span/180 was drawn with a vertical line in the graphs of Figure 8 to ensure the specimens are not in a significant non-linear region at service loads. It also indicates that the ultimate capacity of the specimens is well beyond of the service load. The load-strain and load-deflection curves are, of course, linear up to a point. However, a non-linearity shows up after the linear portion. The main source of non-linearity in the material non-linearity of flax FRP facings in tension and compression, which will be discussed more in-depth in the analytical section. Overall, the specimens with B and C flutes meet the criteria and those with C flute are the most promising configuration for further studies. Per Table 2, C flute has the lowest bulk density amongst all three flutes. This means C flute is the best configuration with the lowest weight and the highest strength and stiffness. It should be noted that C flute is the most common cardboard in the packing industry, which makes it the best option for sandwich applications.

3.5. Flexural and Shear Stiffness

Per ASTM D7250 [29], by comparing the initial stiffness of two span lengths of each group of specimens, the flexural stiffness D and the shear stiffness U can be calculated by the equation below where K is initial stiffness in N/mm, S is the span length in mm, and L is the loading span in mm as follows [5]:

$$K_i \frac{(2S_i^3 - 3S_i L_i^2 + L_i^3)}{96D} + K_i \frac{(S_i - L_i)}{4U} = 1 \tag{1}$$

where i = 1 denotes the parameters to the short-span specimens (S=150 mm), and i = 2 to the long-span specimens (S=300 mm). The first term in the equation is related to flexural deformation and the second term to shear deformation. With having an equation for each span length (i.e. two

equations for each flute), the two parameters of D and U can be calculated [5][29]. It should be highlighted that the ASTM methods are limited to sandwich beams exhibiting linear force-deflection response. As a result, the initial linear region of load-deflection curves was used to determine the initial stiffness K of each specimen. Table 4 shows the calculated values for D and U as well as an experimental value of D based on moment-curvature behavior. It should be noted that the flexural stiffness based on moment-curvature presented in Table 4 is the average from the short and long specimens.

3.6. Core Shear Modulus

Based on the shear stiffness U, the shear modulus G of each core can be calculated as follows:

$$G = \frac{U(h - 2t)}{(h - t)^2 b} \tag{2}$$

where b is the width of the sandwich beam, t is the skin thickness, and h is the height of the entire sandwich beam. All dimensions have units of mm for further calculations. As shown in Table 3, the shear modulus of cores with B, C, and BC flutes was calculated 127, 122, and 195 MPa.

Sadeghian et al. [5] previously studied the properties of sandwich beams manufactured with GFRP skins and 25.75 mm thick polypropylene (PP) honeycomb core with the bulk density of 91 kg/m^3 before applying resin. The PP honeycomb was shown to have the core shear modulus G of 11.4 MPa. In this study, the cardboard B, C, and BC flutes with the bulk density of 170, 127, and 138 kg/m^3 (before applying resin) displayed the shear modulus of 127, 122, and 195 MPa; respectively. The results indicate that the corrugated cardboard cores used in this study had an average shear modulus of almost 13 times that of the PP honeycomb, however the average bulk density of the cardboards was only 60% more than that of the PP honeycomb. The higher stiffness of the corrugated cardboard core may be due to the fact that it is stretch-dominated and the honeycomb core is bending-dominated. It has been shown that cellular cores can deform by either

the bending or stretching of the cell walls [30]. In bending-dominated cells, like honeycombs, the walls of a cell bend due to in-plane loading, however in stretching-dominated cells, like the corrugated cardboards, cells are triangular shape and the walls of a cell form a strut-tie system stretching the walls in tension and compression.

4. ANALYTICAL STUDY

4.1. Theoretical Flexural Stiffness

A theoretical calculation of the flexural stiffness of the sandwich beams tested earlier is presented in this section. It is assumed that all three layers are perfectly bonded together so the sandwich beam acts under full-composite behavior. The cross-section has a width b and total thickness h. Each skin has thickness t and the two skins are separated by a relatively thick core of thickness c. Therefore, its flexural stiffness D is the sum of the flexural stiffness of both skins and the core, measured about the centroidal axis of the cross-section as follows [31][32]:

$$D = E_f \frac{bt^3}{6} + E_f \frac{btd^2}{2} + E_c \frac{bc^3}{12} \tag{3}$$

where E_f and E_c are the modulus of elasticity of skin and core, respectively, and d is the distance between the center lines of the upper and lower skins. The theoretical flexural stiffness of each sandwich group with different cardboard flute was calculated and presented in Figure 10. The theoretical values are compared with the experimental values obtained using both ASTM method and moment-curvature method. As the ASTM method uses deflections and the moment-curvature method uses strains, they do not necessarily result in the same values. The theoretical method is also independent of the experimental values. The figure indicates that the theoretical method can predict the flexural stiffness of the sandwich beams made of the corrugated cardboard core and flax FRP skins. The agreement also indicates that shear deformation of the sandwich specimens in

comparison with flexural deformation is negligible. As the shear deformation of typical sandwich composites with soft cores has negative effect on structural properties, failure load, and design criteria; having a lightweight core such as the cardboards studied in this research with limited negative effect of soft cores is a very promising option for strong, stiff, and lightweight sandwich structures.

4.2. Parametric Study

In this section, a parametric study is performed to evaluate the structural properties of large-scale sandwich beams made of the corrugated cardboard core and flax FRP skins. The second author has previously used foam cores with bidirectional flax FRP skins [7]. The sandwich beams are considered with 75 mm thick and 150 mm wide cores. The flax FRP skins are made of 1, 2, and 3 layers of the bidirectional flax FRP with an elastic modulus of 7500 MPa. Figure 11 presents the comparison of the theoretical flexural stiffness of sandwich beams with C flute (150 mm wide and 75 mm thick core) with the experimental results of similar sandwich beams made of foam cores and flax FRP skins. The figure indicates that the potentials of the cardboard cores. The next stage of the current research program will be testing of the large-scale sandwich beams with cardboard cores under static and impact loading. The results will be used for development of a design procedure for cardboard core sandwich panels for walls and roofs of building under static loadings and dynamic effects due to the impact of a flying object during high wind, hurricane, and tornado.

4.3. Non-Linear Modeling

In this section, a non-linear cross-sectional analysis is presented to predict the load-strain behavior of the sandwich specimens. The non-linearity is a material non-linearity of flax FRP skins as shown in multiple studies [5][6][7][28]. In this study, a parabolic stress-strain curve for flax FRPs in tension is proposed. The model is verified against tests data presented in Figure 12. With the

assumption of linear and symmetric strain profile with respect to the centroidal axis, the strain of top and bottom skins is predicted at any given load. Figure 13 compares the top and bottom skin strains obtained from proposed non-linear model and test data of long and short specimens made of C flute cardboard sheets. Also, a linear model based on initial elastic modulus of flax FRPs are presented in the figure.

As shown in Figure 13(a), both linear and non-linear models can predict the linear regions of the load-strain curves, however after a load about 30% of the peak load, only the non-linear model is able to predict the experimental behavior. The non-linear model can predict the tensile strain at bottom skin very well, however the experimental compressive strain at top skin deviates from the non-linear model at a load about 60% of the peak load. This might be explained by a higher level of non-linearity if flax FRPs in compression. This is compatible with the fact that the sandwich specimens failed under crushing of top skins. Figure 13(b) shows the same trend for short specimens, however both linear and non-linear models slightly under predict the initial stiffness of the sandwich beams. This might be related to the fact that very short specimens do not behave according to the ordinary bending theory. For future studies, a higher-order beam theory is recommended to capture the actual behavior sandwich composites made of cardboard core and flax FRP skins.

5. CONCLUSION

In this study, three different flutes of corrugated cardboard cores, namely B, C and BC flutes, and flax FRP skins and were used to manufacture composite sandwich beams. A total of 30 small-scale sandwich beam specimens were manufactured across six unique beam varieties with dimensions of 50 mm in width, 25 mm in depth, and 200 and 350 mm in length (150 mm and 300 mm spans)

and tested under four-point bending up to failure. The load-deflection behavior, load-strain behavior, and moment-curvature behavior of the sandwich beam specimens were employed to study the effect of each cardboard flute to the strength and stiffness of the system. The flexural and shear stiffness of the sandwich beams were quantified and the results were used to calculate the shear modulus of the cardboards. Also, an analytical study was successfully implemented to predict the flexural stiffness of the sandwich specimens. The following conclusions can be drawn from this study:

- Two failure modes of transverse indentation and longitudinal crushing of the core were observed. All short specimens failed by core indentation, which was followed by indentation of the top skin. However, the long specimens reached a significantly lower peak load and failed by longitudinal crushing of the core due to compressive bending stresses, which caused the top skin to be crushed after the peak load.

- B and C flutes performed much better than BC flute in terms of load carrying capacity. Also, the B and C flutes showed enough strength and stiffness in shear to develop a significant level of tensile and compressive strains close to those of flax FRP skins. The specimens with flute C exhibited a higher flexural stiffness and strength than those with B and BC flutes.

- C Flute with the lowest bulk density and the highest availability in the market amongst all three flutes was selected as the best configuration with the highest strength and stiffness for sandwich applications.

- The corrugated cardboard cores used in this study showed an average shear modulus of almost 13 times that of a polypropylene honeycomb with the same thickness and only 40% lower bulk density.

- The analytical model based on full-composite action was able to predict the flexural stiffness of the sandwich beams made of the corrugated cardboard core and flax FRP skins with a very good agreement with the test results. It indicated that the shear deformation of the core was negligible indicating that the cardboards are a viable option for strong, stiff, and lightweight sandwich structures.

- A non-linear cross-sectional model was developed based on non-linearity of flax FRPs. The model was able to predict the non-linearity of load-strain curves of bottom skin obtained from the experimental program. A more in-depth modeling considering non-linearity of flax FRPs in compression and higher-order beam theory is recommended for the future.

- Although more research must be conducted on large-scale specimens under static and dynamic loading, the all-natural flax FRP and corrugated cardboard sandwich beams displayed encouraging structural behavior and may prove to be a sustainable and structurally efficient building material.

6. ACKNOWLEDGEMENTS

7. REFERENCES

[1] Reis EM, Rizkalla SH. Material characteristics of 3-D FRP sandwich panels. Construction and Building Materials. 2008 Jun 30;22(6):1009-18.

[2] Sharaf T, Shawkat W, Fam A. Structural performance of sandwich wall panels with different foam core densities in one-way bending. Journal of Composite Materials. 2010 Sep;44(19):2249-63.

[3] Manalo A, Aravinthan T, Fam A, Benmokrane B. State-of-the-art review on FRP sandwich systems for lightweight civil infrastructure. Journal of Composites for Construction. 2016 Jul 5;21(1):04016068.

[4] Dweib MA, Hu B, O'donnell A, Shenton HW, Wool RP. All natural composite sandwich beams for structural applications. Composite structures. 2004 Feb 29;63(2):147-57.

[5] Sadeghian P, Hristozov D, Wroblewski L. Experimental and analytical behavior of sandwich composite beams: Comparison of natural and synthetic materials. Journal of Sandwich Structures & Materials. 2018 Mar. 1; 20 (3):287–307.

[6] CoDyre L, Mak K, Fam A. Flexural and axial behaviour of sandwich panels with bio-based flax fibre-reinforced polymer skins and various foam core densities. Journal of Sandwich Structures & Materials. 2016 Dec 5:1099636216667658.

[7] Betts D, Sadeghian P, Fam A. Structural Behaviour of Sandwich Panels Constructed of Foam Cores and Flax FRP Skins. Canadian Society for Civil Engineering (CSCE) Annual Conference, May 31 – Jun. 3, 2017, Vancouver, BC, Canada.

[8] Mathieson H, Fam A. Static and fatigue behavior of sandwich panels with GFRP skins and governed by soft-core shear failure. Journal of Composites for Construction. 2013 Nov 18;18(2):04013046.

[9] Triantafillou TC, Gibson LJ. Failure mode maps for foam core sandwich beams. Materials Science and Engineering. 1987 Nov 1;95:37-53.

[10] Petras A, Sutcliffe MP. Failure mode maps for honeycomb sandwich panels. Composite structures. 1999 Apr 1;44(4):237-52.

[11] Wambua P, Ivens J, Verpoest I. Natural fibres: can they replace glass in fibre reinforced plastics? Composites Science and Technology. 2003 Jul 31;63(9):1259-64.

[12] Yan L, Chouw N, Jayaraman K. Flax fibre and its composites–a review. Composites Part B: Engineering. 2014 Jan 31;56:296-317.

[13] Hristozov D, Wroblewski L, Sadeghian P. Long-term tensile properties of natural fibre-reinforced polymer composites: comparison of flax and glass fibres. Composites Part B: Engineering. 2016 Jun 15;95:82-95.

[14] Ray D, Sarkar BK, Basak RK, Rana AK. Thermal behavior of vinyl ester resin matrix composites reinforced with alkali-treated jute fibers. Journal of Applied Polymer Science. 2004 Sep 15;94(1):123-9.

[15] Faruk O, Bledzki AK, Fink HP, Sain M. Biocomposites reinforced with natural fibers: 2000–2010. Progress in polymer science. 2012 Nov 30;37(11):1552-96.

[16] Wroblewski L, Hristozov D, Sadeghian P. Durability of bond between concrete beams and FRP composites made of flax and glass fibers. Construction and Building Materials. 2016 Nov 15;126:800-11.

[17] Mohanty AK, Misra M, Drzal LT. Sustainable bio-composites from renewable resources: opportunities and challenges in the green materials world. Journal of Polymers and the Environment. 2002 Apr 1;10(1):19-26.

[18] McSwiggan C, Fam A. Bio-based resins for flexural strengthening of reinforced concrete beams with FRP sheets. Construction and Building Materials. 2017 Jan 30;131:618-29.

[19] Loong ML, Cree D. Enhancement of Mechanical Properties of Bio-Resin Epoxy/Flax Fiber Composites using Acetic Anhydride. Journal of Polymers and the Environment. 2018 Jan 1;26(1):224-34.

[20] Gupta N, Woldesenbet E. Characterization of flexural properties of syntactic foam core sandwich composites and effect of density variation. Journal of composite materials. 2005 Dec;39(24):2197-212.

[21] Wadley HN, Fleck NA, Evans AG. Fabrication and structural performance of periodic cellular metal sandwich structures. Composites Science and Technology. 2003 Dec 31;63(16):2331-43.

[22] Davalos JF, Qiao P, Xu XF, Robinson J, Barth KE. Modeling and characterization of fiber-reinforced plastic honeycomb sandwich panels for highway bridge applications. Composite structures. 2001 Jun 30;52(3):441-52.

[23] Aboura Z, Talbi N, Allaoui S, Benzeggagh ML. Elastic behavior of corrugated cardboard: experiments and modeling. Composite structures. 2004 Jan 1;63(1):53-62.

[24] von der Heyden A, Lange J. Assessment of the utilisation of corrugated cardboard as a core material for sandwich panels. ce/papers. 2017 Sep 1;1(2-3):1716-25.

[25] Paper and Paperboard Packaging Environmental Council. Factsheet 03-2017. http://www.ppec-paper.com/pdfFiles/factsheets/2017/Packaging/FS03-2017.pdf

[26] Kandare E, Luangtriratana P, Kandola BK. Fire reaction properties of flax/epoxy laminates and their balsa-core sandwich composites with or without fire protection. Composites Part B: Engineering. 2014 Jan 31;56:602-10.

[27] Osei-Antwi M, De Castro J, Vassilopoulos AP, Keller T. Shear mechanical characterization of balsa wood as core material of composite sandwich panels. Construction and Building Materials. 2013 Apr 30;41:231-8.

[28] Betts D, Sadeghian P, Fam A. Tensile Properties of Flax FRP Composites. In 6th Asia-Pacific Conference on FRP in Structures (APFIS 2017) 2017 Jul 19. 6th Asia-Pacific Conference on FRP in Structures, Singapore.

[29] ASTM D7250. Standard practice for determining sandwich beam flexural and shear stiffness. West Conshohocken, PA, USA: ASTM International, 2012.

[30] Deshpande VS, Ashby MF, Fleck NA. Foam topology: bending versus stretching dominated architectures. Acta materialia. 2001 Apr 2;49(6):1035-40.

[31] Zinno A, Bakis CE, Prota A. Mechanical characterization and structural behavior of composite sandwich structures for train applications. In Proceedings of the 8th international conference on sandwich structures (ICSS8), 2008 May 6, Vol. 1, pp. 570-581, Berlin: Springe.

[32] Allen, HG. Analysis and design of structural sandwich panels. 1969, Pergamon Press, Oxford, UK.

Table 1. Test Matrix.

Case #	Specimen ID	Cardboard flute	Span (mm)
1	B-S150	B	150
2	B-S300	B	300
3	C-S150	C	150
4	C-S300	C	300
5	BC-S150	BC	150
6	BC-S300	BC	300

Note: three identical specimens per case were prepared and tested.

Table 2. Cardboard flute comparison.

Cardboard flute	Thickness (mm)	Flutes per meter length	Bulk density (kg/m^3)
B	2.8	160	170
C	4.0	120	127
BC	6.6	Mix	138

Table 3. Summary of test results.

Specimen group ID	Peak Load (N)		Initial stiffness (N/mm)		Peak moment (N-m)		Curvature at peak (1/km)		Flexural stiffness (N-m^2)		Failure Mode
	AVG	SD	AVG	SD	AVG	SD	AVG	SD	AVG	SD	
B-S150	3587	279	2671	9.0	110.1	8.6	1003	164	257	22	Indentation
B-S300	1493	13	252	12.1	91.6	0.8	1163	136	173	14	Crushing
C-S150	3985	297	2209	154.6	122.3	9.1	953	188	231	10	Indentation
C-S300	1715	201	387	27.1	105.2	12.4	1168	208	215	21	Crushing
BC-S150	1881	297	2089	336.4	57.7	9.1	564	254	209	29	Indentation
BC-S300	917	161	329	26.8	56.3	9.9	677	72	175	10	Crushing

Note: AVG = average; and SD = standard deviation.

Table 4. Flexural and shear stiffness of cardboard sandwiches.

Cardboard flute	Flexural stiffness, D (N-m^2)		Shear stiffness, U (kN)	Shear modulus, G (MPa)
	ASTM method	Moment-curvature slope		
B	127.1	215.3	192.4	127.0
C	242.9	223.3	182.9	121.9
BC	197.0	191.9	271.6	194.9
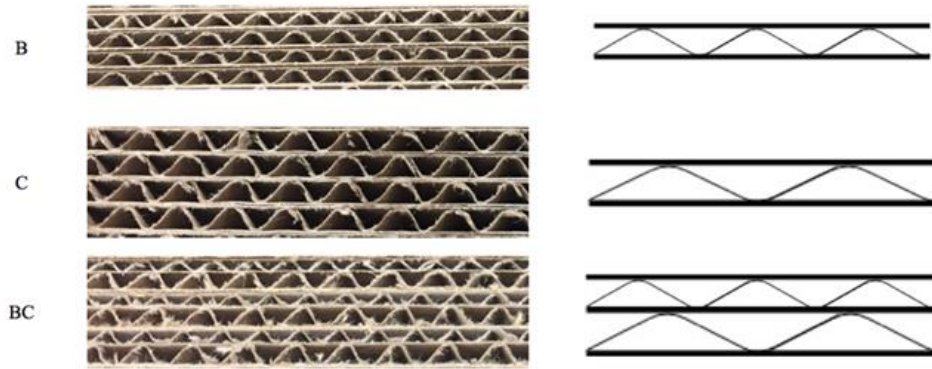
Figure 1. Visual comparison of cardboard sheets with B, C, and BC flutes.
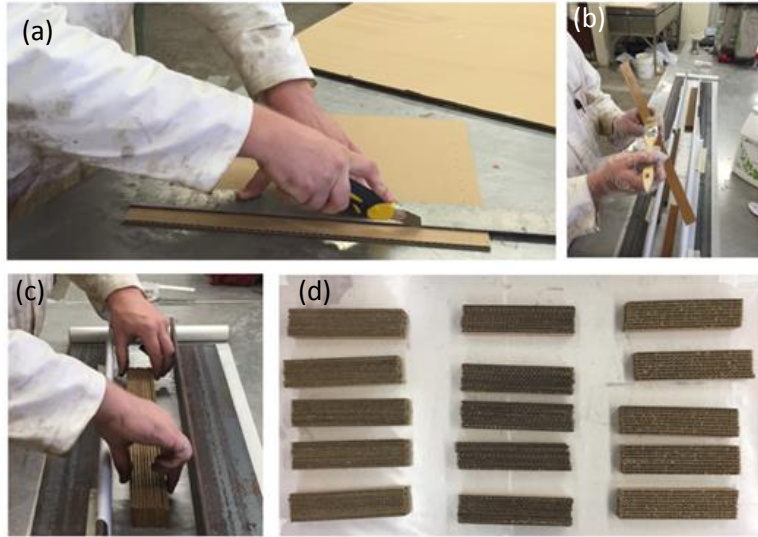
Figure 2. Cardboard core fabrication: (a) cutting; (b) applying adhesive; (c) combining into one core; and (d) completed cores for 150 mm span.
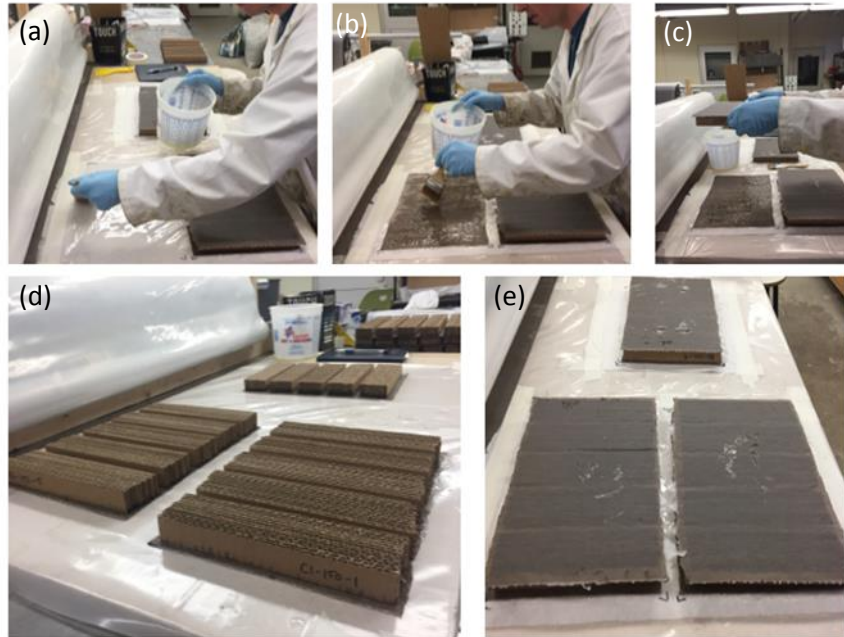
Figure 3. Specimen fabrication: (a) applying epoxy; (b) saturating flax fabric; (c) placing cardboard cores on saturated fabric; (d) first side complete; and (e) both sides complete.
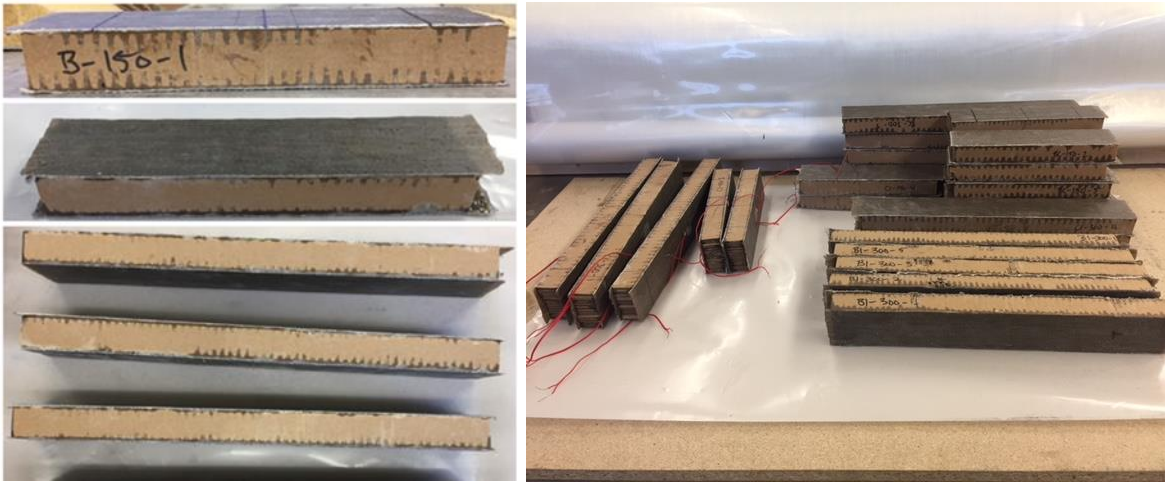
Figure 4. Sandwich beam specimens before and after strain gauging.
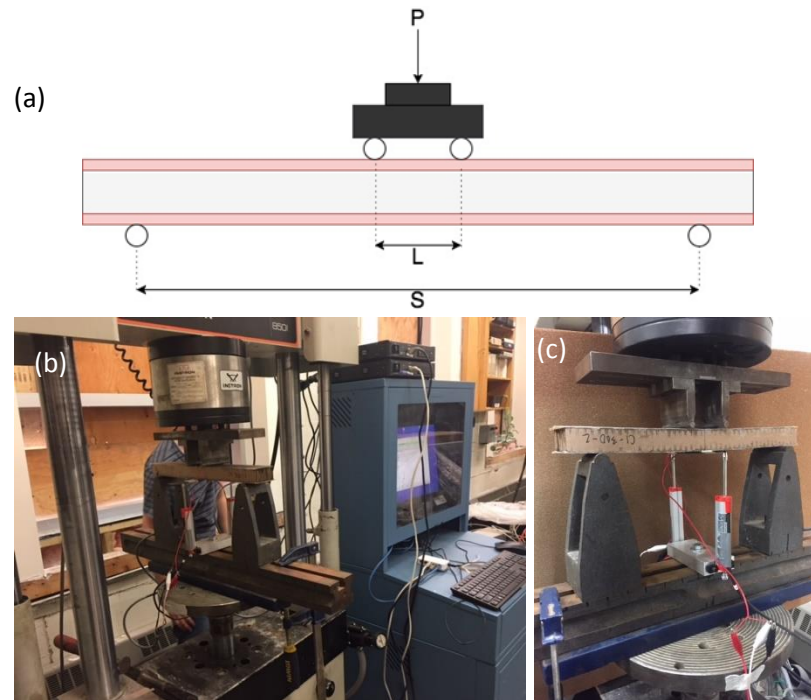
Figure 5. Test setup and instrumentation: (a) four-point bending schematic; (b) testing machine and data acquisition system; and (c) specimen ready for testing.
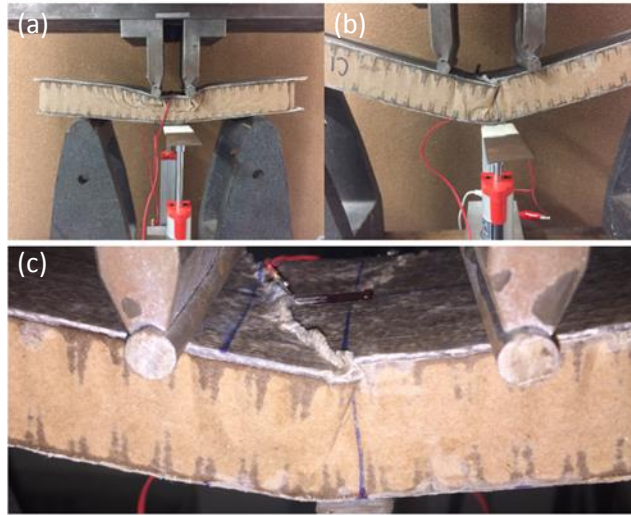
Figure 6. Failure modes: (a) indentation; (b) longitudinal crushing; and (c) detail of top skin crushing.
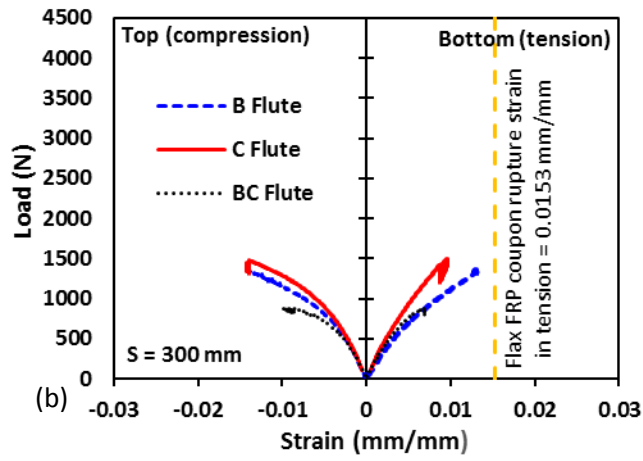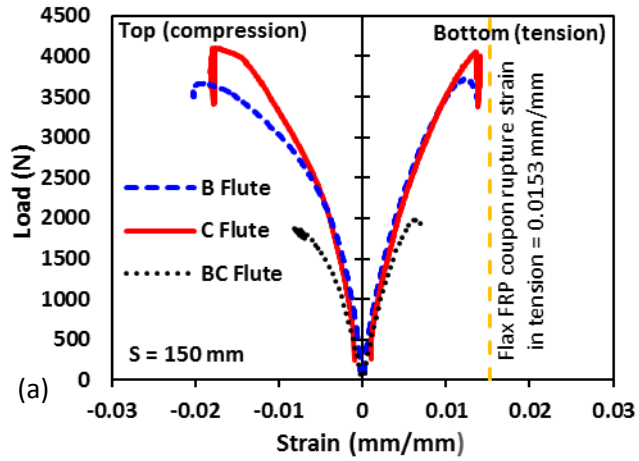
**Figure 7. Load-strain behavior of specimens: (a) 150 mm span; and (b) 300 mm span (note: each curve is the average of three identical specimens).**
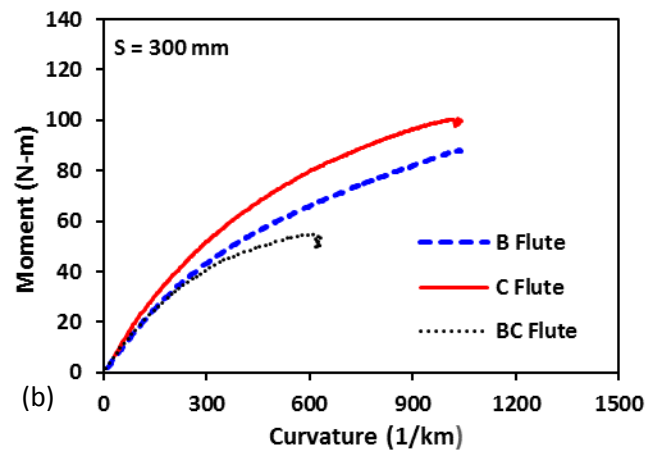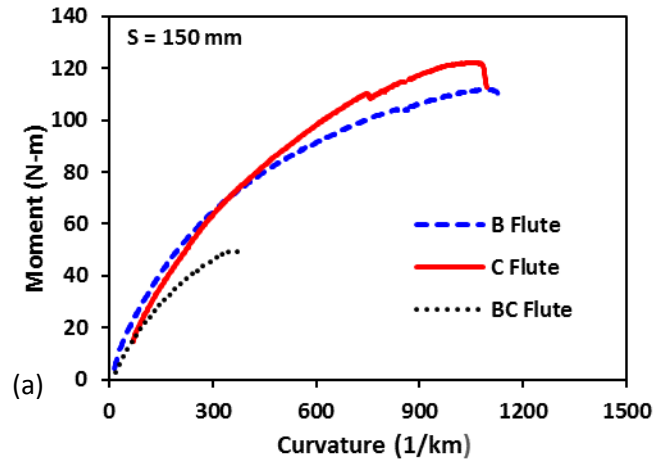
Figure 8. Moment-curvature behavior of specimens: (a) 150 mm span; and (b) 300 mm span (note: each curve is the average of three identical specimens).
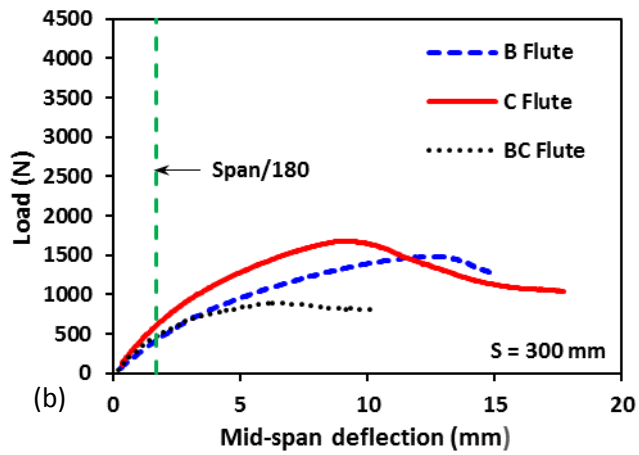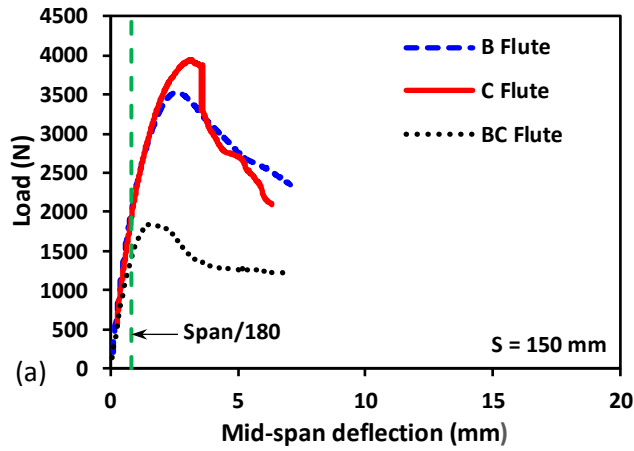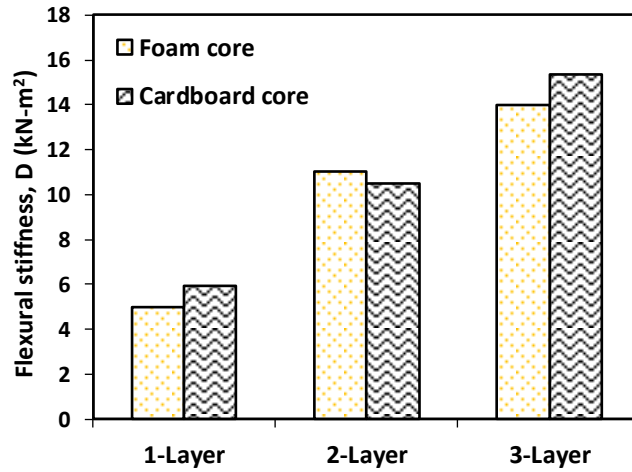
Figure 9. Load-deflection behavior of specimens: (a) 150 mm span; and (b) 300 mm span (note: each curve is the average of three identical specimens).
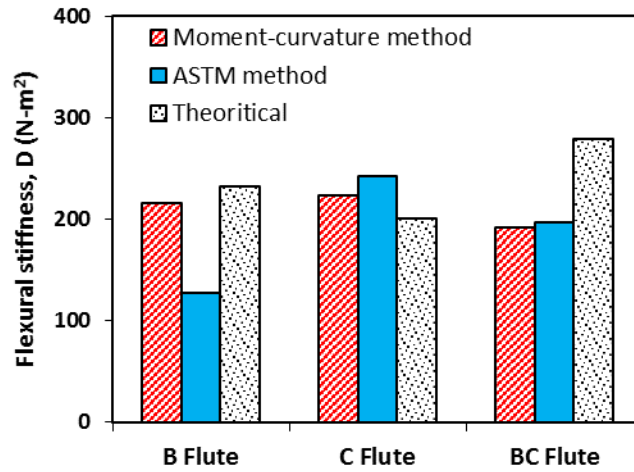
Figure 10. Comparison of theoretical and experimental flexural stiffness of sandwich beams with cardboard B, C, and BC flutes.

Figure 11. Comparison of theoretical flexural stiffness of sandwich beams with cardboard C flute (150 mm wide and 75 mm thick core) with experimental results of similar foam cores and flax FRP skins.
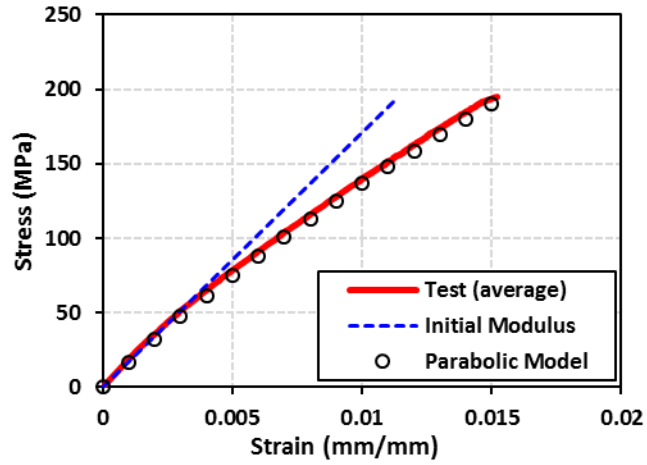
Figure 12. Proposed parabolic stress-strain behaviour of flax FRPs in comparison with coupon test data adopted from Betts et al. [28]
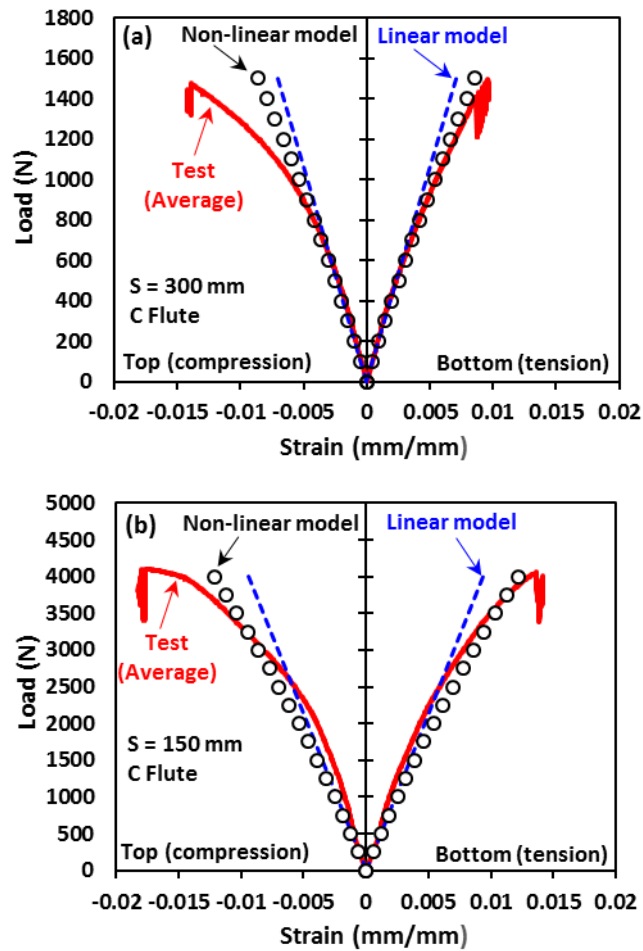
Figure 13. Comparison of top and bottom skin strains obtained from proposed non-linear model and test data: (a) long specimens; (b) short specimens made of C flute cardboard sheets.